Analysis of Vinylene Carbonate (VC) as Additive in Graphite/LiNi$_{0.5}$Mn$_{1.5}$O$_4$ Cells

Daniel Pritzl,[*,z] **Sophie Solchenbach,**[*] **Morten Wetjen, and Hubert A. Gasteiger**[**]

Chair for Technical Electrochemistry, Department of Chemistry and Catalysis Research Center, Technical University of Munich, Munich, Germany

Vinylene Carbonate (VC) is an effective electrolyte additive to produce a stable solid electrolyte interphase (SEI) on graphite anodes, increasing the capacity retention of lithium-ion cells. However, in combination with LiNi$_{0.5}$Mn$_{1.5}$O$_4$ (LNMO) cathodes, VC drastically decreases cell performance. In this study we use on-line electrochemical mass spectrometry (OEMS) and electrochemical impedance spectroscopy (EIS) with a micro-reference electrode to understand the oxidative (in-)stability of VC and its effect on the interfacial resistances of both anode and cathode. We herein compare different VC concentrations corresponding to VC to graphite surface area ratios typically used in commercial-scale cells. At low VC concentrations (0.09 wt%, corresponding to 1 wt% in commercial-scale cells), an impedance increase exclusively on the anode and an improved capacity retention is observed, whereas higher VC concentrations (0.17 wt – 2 wt%, corresponding to 2 wt - 23 wt% in commercial-scale cells) show an increase in both cathode and anode impedance as well as worse cycling performance and overcharge capacity during the first cycle. By considering the onset potentials for VC reduction and oxidation in graphite/LNMO cells, we demonstrate that low amounts of VC can be reduced before VC oxidation occurs, which is sufficient to effectively passivate the graphite anode.

During the first charge of a lithium ion battery (LiB), the so called solid electrolyte interphase (SEI)[1] is formed on the surface of the negative electrode. The standard electrolyte for LiBs consists of a mixture of cyclic and linear carbonates, e.g., ethylene carbonate (EC) and ethyl methyl carbonate (EMC), typically with lithium hexafluorophosphate (LiPF$_6$) as salt. Starting from a potential of ~0.8 V vs. Li/Li$^+$, EC is reduced electrochemically into ethylene gas and lithium ethylene dicarbonate (LEDC), which is a key component of the SEI.[2,3] Vinylene carbonate (VC) is one of the most effective additives to modify the SEI on graphite anodes, as it is reduced at potentials more positive than 1.0 V vs. Li/Li$^+$ and hence suppresses the reduction of EC.[4,5] Aurbach et al. have used VC as electrolyte additive in an EC/DMC (dimethyl carbonate) based electrolyte and that time reported a reduction of the irreversible capacity in the first cycles and an improved cycling stability at elevated temperatures for graphite anodes. The SEI resulting from the reduction of VC consists mainly of poly (vinylene carbonate) (poly(VC)).[4,6]

Important studies on the impact of different VC concentrations in graphite/NMC pouch cells have been carried out by the Dahn group. For example, Burns et al.[7] investigated the effect of different concentrations of VC (0, 1 and 2 wt%) on cycle life and impedance growth of full-cells with graphite anodes and either LCO (LiCoO$_2$) or NMC (Li(Ni$_{0.42}$Mn$_{0.42}$Co$_{0.16}$)O$_2$) cathodes, employing galvanostatic cycling experiments coupled with high precision coulombic efficiency and electrochemical impedance spectroscopy (EIS) measurements. For cells with VC additive, they observed higher coulombic efficiencies and reduced capacity fading, whereby a notable increase in cell impedance was observed for cells with 2 wt% VC, which they attributed to a thicker SEI-film at the surface of the anode. However, since it is known that LCO cathodes can also form a resistive surface film in the presence of VC additive (presumably consisting of poly(VC)[8,9]), an assignment of the overall cell impedance growth to the individual contributions from anode and cathode requires more advanced techniques, like the symmetric cell approach.[10] Thus, later on, Burns et al.[10] investigated the effect of VC (0 - 6 wt%) over extended charge/discharge cycling of graphite/NMC 18650 cells on anode and cathode impedance growth via symmetric cell measurements. They

showed that indeed the impedance of the negative electrode increases nearly linearly with VC concentration, whereas the impedance of the positive electrode first decreases as the VC concentration is increased to 2 wt% and then only increases gradually at higher VC concentrations. The strong anode impedance growth suggests that VC is mostly consumed at the graphite anode, leading to SEI growth. This is consistent with a study by Petibon et al.,[11] who analyzed the consumption of vinylene carbonate in graphite/NMC pouch cells and showed that the additive is mainly consumed at the anode side (both during high temperature formation (50°C) and during a potential hold at 4.2 V cell voltage). In addition, they found that nearly 2 wt% VC were consumed during formation, so that little residual VC remained after formation for VC concentrations of ≤2 wt%. In a subsequent study, Petibon et al.[12] also showed that residual VC after formation leads to a fast decay in the open-circuit voltage during storage in cells charged to 4.4 V cell voltage, caused by the poor oxidative stability of VC.

In a recent study from our group,[13] we compared the effect of different VC concentrations on the impedance of graphite anodes in graphite/LFP (LiFePO$_4$) full-cells, using a Swagelok T-cell configuration with a reference electrode which enables the deconvolution of the overall cell impedance into the individual contributions from anode and cathode. There, we showed that the VC to active material ratio (expressed as the ratio of VC mass to graphite surface area in the cell), rather than the concentration of the additive in the electrolyte, is a key parameter when comparing results using different types of battery cell hardware. Basically, the cell hardware can roughly be categorized either into lab-scale-cells with a small total capacity (<10 mAh, i.e., <5 cm^2 electrode area), which due to design constraints require a high electrolyte/active material mass ratio in order to function properly (e.g., coin or Swagelok T-cells), or into commercial-scale cells with a high total capacity (>100 mAh, i.e., >20 cm^2 electrode area), which are assembled with much lower electrolyte/active material mass ratios (e.g., multi-layer pouch or 18650 cells with low electrolyte/active material mass ratio). Consequently, the electrolyte/active material mass ratio in the latter is ~12-fold lower compared to commonly used lab-scale cells, so that a concentration of 2 wt% VC in the study from Burns et al.[10] based on 18650 cells would corresponds to ~0.17 wt% VC in a typical lab-scale cell. This scaling factor between commonly used lab-scale cells and commercial-scale cells needs to be considered when using lab-scale cells to evaluate the effect of additives.

*Electrochemical Society Member.
**Electrochemical Society Fellow.
zE-mail: daniel.pritzl@tum.de

While the above discussed studies show that the cathode impedance growth with VC additive is generally small for graphite/LCO and graphite/NMC cells operating at cell voltages up to 4.4 V, this is not the case when higher voltage cathode active materials such as high-voltage spinel $LiNi_{0.5}Mn_{1.5}O_4$ (LNMO) are used. Li et al.[14] have shown that the cell performance of graphite/LNMO cells drastically decreases when 1 or 2 wt% of VC are added to the electrolyte, consistent with studies by Lee et al.[15] and Song et al.,[16] which demonstrated that the oxidative stability of VC is insufficient for operation with an LNMO cathode. The oxidative instability of VC was examined in more detail in a recent study from the group of Brett Lucht:[17] By means of ex-situ surface analysis (XPS and FT-IR) they showed that the oxidation of VC starts at already ∼4.5 V vs. Li/Li$^+$, leading to the formation of poly(VC) at the surface of the LNMO cathode. Even though these studies demonstrate that VC is not a suitable additive for cells with LNMO cathodes, they were all based on lab-scale cell setups with a high electrolyte/active material ratio, so that the ratio of VC mass over graphite surface area for the used VC concentrations of 1–2 wt% was roughly an order of magnitude higher than what would be present in commercial-scale cells.

The additive VC behaves very differently in high-voltage cells compared to fluorinated additives. Fluoroethylene Carbonate (FEC) is often used in this type of cells, leading to an overall increased battery performance. On the one hand both additives (VC and FEC) generate CO_2 during reduction,[5,18] thus improving the anode SEI. On the other hand, FEC is more stable towards oxidation[19] (compared to VC) and can thus be used in large concentrations/quantities even at high voltages (e.g., with LNMO or HE-NCM cathodes).

In the present study, we therefore want to investigate much lower VC concentrations in the electrolyte in lab-scale cell tests (0.09–0.52 wt% VC), which would correspond to VC concentrations of 1–6 wt% in commercial-scale cells for the same ratio of VC mass to graphite surface area. The first part of our investigation aims to understand the drastic decrease in cell performance when large amounts of VC are added to graphite/LNMO cells (i.e., at very high ratios of VC mass to graphite surface area). To this end, we will examine the anodic stability of VC via on-line electrochemical mass spectrometry (OEMS) using carbon black model electrodes and a VC-only electrolyte with 1 M LiPF$_6$. As a next step, we conduct impedance measurements in graphite/LNMO cells using a micro-reference electrode,[13] quantifying anode and cathode impedance after formation in electrolytes with different amounts of VC (0.09, 0.17, 0.52, and 2 wt%). In the second part, we examine the impact of different VC concentrations on the cycling behavior of graphite/LNMO cells and on anode/cathode impedance during cycling at 40°C. We also show that the additional capacity during the first charge correlates with the impedance of the LNMO cathode. Finally, by comparing the impedance growth of the graphite anode in cells with either an LNMO or an LFP cathode, we can clearly show that VC is consumed at the LNMO cathode, resulting in a lower impedance of the of the graphite anode in a graphite/LNMO vs. a graphite/LFP cell.

Experimental

Electrode preparation.—$LiNi_{0.5}Mn_{1.5}O_4$ (LNMO) electrodes were prepared by mixing LNMO (BASF SE, Germany), carbon black (Super C65, Timcal), and polyvinylene difluoride (PVDF, Kynar) at a mass ratio of 92/5/3 with NMP (N-methyl pyrrolidone, anhydrous, Sigma-Aldrich, Germany) in a planetary mixer (Thinky Corp.) for 15 min. The ink was coated onto aluminum foil (MTI, 18 μm) with a doctor blade coater and dried afterwards at 50°C in a convection oven for at least 3 h. The final LNMO coating had a loading of ∼13.6 mg$_{LNMO}$/cm^2, corresponding to ∼1.9 mAh/cm^2. Electrodes with a diameter of 11 mm (≡0.95 cm^2) were punched out and compressed to ∼30% porosity with a KBr press. Graphite electrodes were prepared by mixing graphite (T311, SGL Carbon, Germany) and PVDF at a mass ratio of 95/5 with NMP by applying the same procedure as for the positive electrodes. The graphite ink was coated onto copper foil (MTI, ∼12 μm) and dried in a convection oven at 50°C for 3 h. The

loading of the graphite coating was ∼7 mg$_{graphite}$/cm^2 corresponding to ∼2.6 mAh/cm^2. The electrodes were punched out with a diameter of 11 mm and compressed to a porosity of ∼30%. Both types of electrodes were dried under dynamic vacuum at 120°C for at least 12 h in a vacuum oven (Büchi, Switzerland) and then transferred into an Argon-filled glove box (MBraun, Germany) without exposure to air.

For OEMS measurements, isotopically labelled ^{13}C-electrodes were prepared by dispersing ^{13}C-carbon (BET ∼140 m^2/g, 99% isotopic purity, Sigma-Aldrich, Germany) in NMP with an ultrasonication horn. PVDF was dissolved in NMP to yield a 10% wt solution. The PVDF solution was added to the ^{13}C-dispersion to yield a final mass ratio of 1:2 (PVDF:^{13}C), and stirred carefully. The ink was then coated onto a polyester separator (Freudenberg, Germany) with a wedge bar and dried in a convection oven at 50°C. Afterwards, electrodes with a diameter of 15 mm were punched out, dried under dynamic vacuum at 120°C over night and transferred into an argon-filled glove box. The final electrodes had a loading of ∼1 mg$_C$/cm^2.

On-line electrochemical mass spectrometry.—The on-line electrochemical mass spectrometry (OEMS) setup has been described in more detail in a previous publication by our group.[20] For the experiments in this study, we used a recently developed sealed 2-compartment cell,[21] where working and counter electrode are separated by a sealed lithium-ion conductive glass ceramics (Ohara Corp., Japan). In this way, only gases coming directly from the working electrode are detected, and any gas evolution related to the lithium counter electrode or electrode crosstalk can be avoided. The cells were assembled with a lithium counter electrode (Ø 17 mm, 450 μm thickness, Rockwood Lithium, USA), a glassfiber separator soaked with 250 μL electrolyte in the lower compartment and a polyester separator soaked with 100 μL electrolyte in the upper compartment. The investigated electrolytes consisted only of EC or VC with 1 M LiPF$_6$ (all from BASF SE, Germany). To distinguish between electrolyte oxidation and carbon corrosion, we used isotopically labelled ^{13}C-carbon electrodes coated on a polyester separator as working electrodes (see above). The oxidative stability of the electrolytes was investigated by a linear potential sweep from OCV (∼3 V vs. Li/Li$^+$) to 5.5 V vs. Li/Li$^+$ at a scan rate of 0.1 mV/s. The quantification of the OEMS signals in terms of moles of produced gas was described previously,[22] and gas evolution rates are reported in terms of μmol gas/m$^2_{BET}$ of the ^{13}C-electrode.

Electrochemical characterization.—Swagelok T-cells with a Gold Wire Reference Electrode (GWRE)[13] were assembled in an argon filled glove box (O$_2$ and H$_2$O < 0.1 ppm, MBraun, Germany) using two glass fiber separators (11 mm diameter, 200 μm thickness, glass microfiber #691, VWR, Germany) and 60 μL of electrolyte. The electrolyte consisted of standard LP57 (1 M LiPF$_6$ in EC: EMC (3:7 wt/wt) < 10 ppm H$_2$O, BASF, Germany) without and with different amounts of vinylene carbonate (VC, BASF SE, Germany), which was added at concentrations of 0.09, 0.17 0.52 and 2 wt% to the electrolyte. The cells were assembled using a graphite anode, a LNMO cathode, and a gold wire reference electrode (GWRE). The detailed experimental procedure for the assembly can be found in Reference 13. For charge/discharge cycling, identical Swagelok T-cells without a reference electrode were assembled. Cell cycling was carried out in a climate chamber (25°C or 40°C, Binder, Germany) with a battery cycler (Series 400, Maccor, USA). The cycling protocol consisted of the following steps: i) two formation cycles with C/10 at 25°C, ii) charge/discharge cycling with 1C (20 cycles) at 40°C, and iii) charge/discharge cycling with 1C/3C (2 cycles) at 40°C. The steps ii) and iii) were repeated five times. All cycles were performed between 3.5 V – 4.8 V cell voltage, using a constant current constant voltage (CCCV) charge with a current limit of C/20 for the constant voltage phase and a constant current (CC) discharge. The C-rate is referenced to the theoretical capacity of the LNMO cathode (140 mAh/g$_{LNMO}$), i.e., 1C corresponds to 140 mA/g$_{LNMO}$. or ∼1.9 mA/cm^2.

Electrochemical impedance spectroscopy (EIS) measurements on graphite/LNMO cells with GWRE were conducted after the first

formation cycle at 50% SOC (charged to 50% SOC with C/10) and after the 22nd, 66th and 102nd (charged to 50% SOC with 1C) using a potentiostat (VMP300, BioLogic, France). Prior to the impedance measurement, the cells were charged to 50% SOC, transferred to a climate chamber set to 10°C, and stored for 1 h in order to ensure a constant temperature of the cells. Galvanostatic electrochemical impedance spectroscopy (GEIS) was used in a frequency range from 100 kHz – 100 mHz with an amplitude of 0.6 mA.

In a previous study[13] we have demonstrated the stability of the GWRE reference potential (0.31 V vs. Li/Li$^+$) in graphite/LFP cells to be >500 h. By replacing the LFP electrode (upper cut off potential ~4.1 V vs. Li/Li$^+$) by a LiNi$_{0.5}$Mn$_{1.5}$O$_4$ electrode (upper cut off potential ~4.9 V vs. Li/Li$^+$), the long-term stability of the GWRE reference potential is limited. The potential drift observed in the latter case might be caused by oxidation products generated at the high-voltage positive electrode (LNMO) and their subsequent reduction at the exposed surface of the gold wire, leading to an oxidation of the lithium-gold alloy (i.e., to its gradual delithiation). To overcome this issue, relithiation of the GWRE (at 150 nA for 1 h, consuming <0.1% of the capacity of the LNMO electrode during each charge) is carried out before each impedance measurement. A similar observation is reported by Klett et al.,[23] who also relithiated their Li$_x$Sn reference electrode prior to each impedance measurement.

Results

Anodic stability of vinylene carbonate (VC) investigated via on-line electrochemical mass spectrometry (OEMS).—Until now, the detrimental oxidation of VC is regarded as a major obstacle for the successful use of VC in LNMO cells.[14–17] In order to investigate the onset potential for VC oxidation and its products, we performed on-line electrochemical mass spectrometry on electrolytes based on only VC or EC mixed with 1 M LiPF$_6$. For these experiments, we used carbon black electrodes made from isotopically labelled ^{13}C-carbon, so that we can track the gas evolution from the unlabeled ^{12}C-electrolyte by monitoring the corresponding ^{12}C-related signals of CO$_2$ and CO.[22] As Jung et al.[24] recently showed that the onset and extent of electrolyte oxidation on LNMO and carbon black is identical, it is safe to transfer the results obtained from the ^{13}C-carbon model electrodes to real LNMO cathodes later on. To avoid crosstalk between oxidized species and the lithium counter electrode, we used our sealed 2-compartment cell setup.[21] In this way, only the direct oxidation of the pure electrolyte is observed. Figure 1 shows the current profile (a) and the gas evolution (b) of ^{12}CO$_2$ (m/z = 44, solid lines) and ^{12}CO (m/z = 28, dotted lines) during an oxidative scan in either EC-only or VC-only electrolytes with 1 M LiPF$_6$ from OCV (~3 V vs. Li/Li$^+$) to 5.3 V vs. Li/Li$^+$. While the current signal includes processes like capacitive currents related to the electrode surface or PF$_6{}^-$ intercalation into the graphitic domains of the conductive carbon, which is reported to start around 4.6 V vs. Li/Li$^+$,[25,26] we believe that the evolution of gaseous electrolyte oxidation products is a more meaningful indicator for the onset of electrolyte oxidation. As expected, Figure 1b shows that the oxidative CO$_2$-release of VC starts at significantly lower potentials (~4.3 V vs. Li/Li$^+$) compared to EC (~4.8 V vs. Li/Li$^+$). The small current starting at ~3.7 V vs. Li/Li$^+$ for VC is most likely related to the oxidation of the BHT stabilizer (butylated hydroxytoluene), as its integration between 3.67 V and 4.0 V yields a charge of 10.2 mAs compared to the 11.9 mAs theoretically needed for the 1-electron oxidation of the 200 ppm BHT contained in VC. Interestingly, there is no CO evolution resulting from the oxidation of VC (See red dotted line in Figure 1b); on the other hand, the electrooxidation of EC yields both CO$_2$ and small amounts of CO (see black dotted lines in Figure 1, bottom panel), as we had discussed previously.[27]

The lower anodic stability of VC compared to EC has already been demonstrated by previous experimental results[15,17,28] and calculations.[29,30] The CO$_2$ evolution from VC at potentials above ~4.3 V vs. Li/Li$^+$ (see Figure 1b), corresponding to ~4.2 V cell voltage in a full-cell with a graphite anode, fits well to the observation made by the Dahn group[11,31–33] that commercials cells containing VC
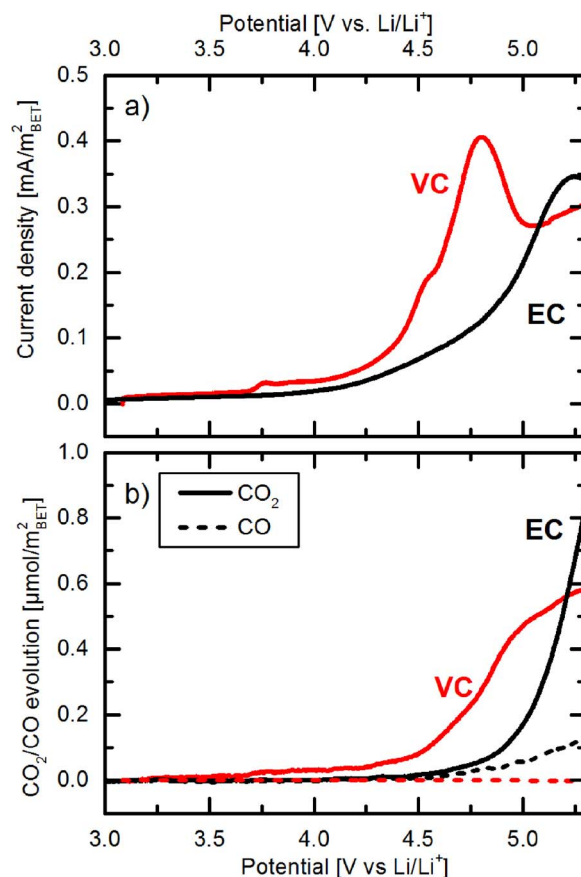

Figure 1. Anodic current (a) and evolution of ^{12}CO$_2$ (b, solid lines) and ^{12}CO (b, dotted lines) from the electrolyte during a linear scan from OCV to 5.3 V vs. Li/Li$^+$ (0.1 mV/s) on a ^{13}C carbon electrode in electrolytes containing only EC (black lines) or VC (red lines) and 1M LiPF$_6$. The experiments were performed using on-line electrochemical mass spectrometry and a sealed 2-compartment cell[21] to avoid crosstalk with the lithium counter electrode.

evolve more gas when held at high potentials compared to the same cells without VC electrolyte. According to the EC oxidation mechanism proposed by Xing et al.[34] and Li et al.,[35] CO$_2$ is readily abstracted after ring opening of the EC radical cation (Scheme 1, black pathway 1a), while the evolution of CO from EC is energetically less favorable and only occurs with a simultaneous breaking of the CH$_2$-CH$_2$ bond after the intial ring opening (see blue pathway 1b in Scheme 1); for further discussion see Ref. 21). Although the decomposition mechanism of EC resulting in CO$_2$ can easily be applied to VC (see black pathway 2a in Scheme 1), the analogous pathway leading to CO is likely to present a very large barrier in the case of VC, as this would require breaking the much stronger CH=CH bond. Hence, our observation that no CO is produced during VC oxidation (Figure 1b) would be consistent with an analogous ring opening reaction as in the case of EC, which disagrees however with the early modeling predictions made by Zhang et al.[5] As poly(VC) has been found on electrodes cycled to high potentials in VC-containing electrolytes,[17] we assume that the radical cations formed in (2a) can trigger a radical polymerization reaction of VC to poly(VC) (see green pathway 2b in Scheme 1).[9,17]

Extracting the interfacial resistance from the impedance spectra.—As a next step, cells with different VC concentrations are assembled and impedance spectra are collected in order to understand the impact of the anodic decomposition of the additive in a graphite/LNMO full-cell. To extract the interfacial resistance from the anode Nyquist plots, the equivalent circuit shown in Figure 2a is used: i) the high frequency resistance (HFR) R_{HFR} represents the
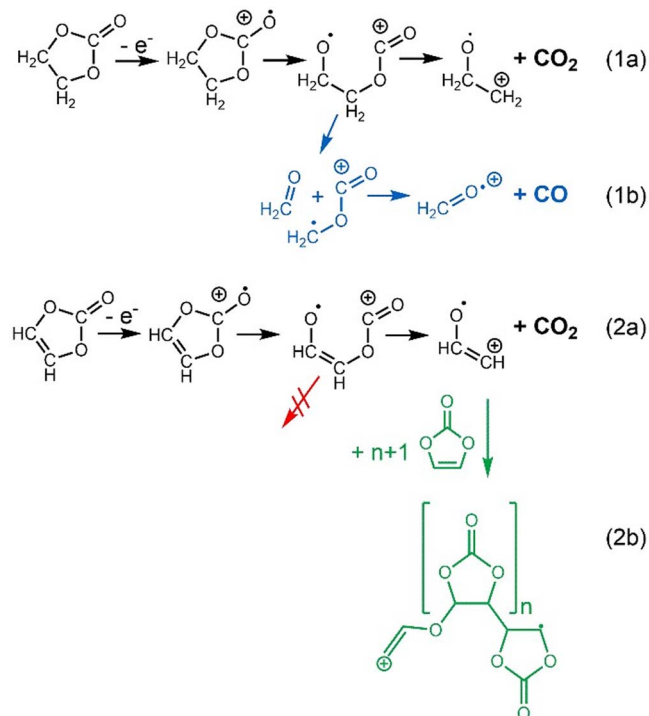
Scheme 1. Oxidation mechanism of EC leading to CO_2 (1a, black) and CO (1b, blue) as proposed by Xing et al.,[34] oxidation mechanism of VC leading to CO_2 (2a, black) and poly(VC) (2b, green).
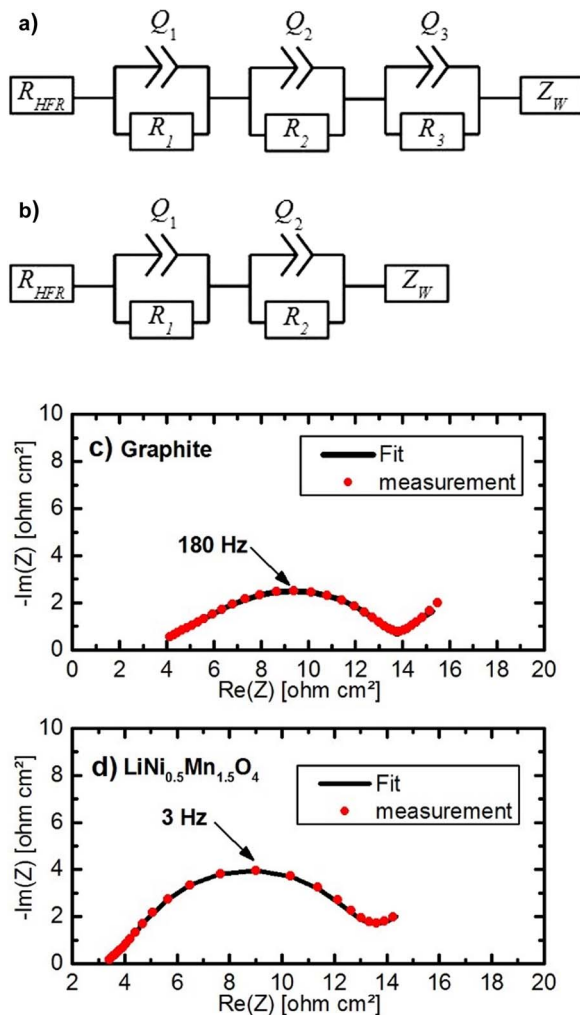

Figure 2. Equivalent circuit models for fitting the anode (a) and the cathode (b) impedance spectra. The Nyquist plots after one formation cycle and recharge to 50% SOC (at 0.1C and 40°C) of graphite/LNMO cells with LP57 electrolyte with 0.09 wt% VC are shown for both the graphite anode (c) and the LNMO cathode (d), whereby the experimental data (red points) are compared to the corresponding fit of the measurement (black line). The impedance is measured from 100 kHz to 100 mHz with an amplitude of 0.6 mA @ 10°C and 50% SOC.

contributions from the ionic conduction in the separator (between the GWRE and the respective electrode) and external electrical contact resistances; ii) up to three RQ-elements (resistor and constant-phase element in parallel) are used to determine the overall resistance of the anode, consisting of contributions from the charge transfer resistance, the solid-electrolyte interphase resistance, and one as yet unknown impedance contribution at low frequencies when high VC concentrations (0.52 and 2 wt%) are used (see Figure 3a); iii) the Warburg element (Z_W) mostly represents the diffusion of lithium in the liquid electrolyte phase as described in Reference 36. For the LNMO cathode, the equivalent circuit shown in Figure 2b is used, representing the analogous processes as in the case of the anode. Since the main focus of this study was to determine the individual impedance growth of anode and cathode during formation and extended charge/discharge cycling, only the overall anode and cathode impedance will be considered in the following ($R_{Anode} = R_1 + R_2 + R_3$, see Figure 2a; $R_{Cathode} = R_1 + R_2$ see Figure 2b). After the 22th cycle, a semi-circle at high frequencies appears in the cathode impedance spectra, which was shown to be due to the formation of a contact resistance at the interface between the cathode electrode and the cathode current collector,[36] and which will be omitted from the fitting process in this study. Unfortunately, a meaningful deconvolution/assignment of the individual impedance contributions to the overall impedance for each electrode would require more elaborate experiments, as we have shown in our recent work for the LNMO cathode impedance.[36] However, as explained above, the main objective of this study was to quantify the individual evolution of anode (R_{Anode}) vs. cathode ($R_{Cathode}$) impedance over extended charge/discharge cycling, for which a deconvolution into the various process is not necessary.

Figures 2c and 2d show exemplary Nyquist plots of a graphite anode and a LNMO cathode after one formation cycle in a graphite/LNMO full-cell with 0.09 wt% VC additive. The red points represent the experimental spectra (100 kHz - 100 mHz, current perturbation of 0.6 mA, 10°C), while the black line represents the fit to the equivalent circuit shown in Figures 2a and 2b. The values for the HFR of anode and cathode are ~4.0 and ~3.5 Ωcm², respectively;

the cause for the slight difference in these HFR values (which are expected to be identical for a symmetric placement of the GWRE) was described elsewhere.[13] The overall resistances of the anode (R_{Anode}) and the cathode ($R_{Cathode}$) are in both cases ~10 Ωcm².

Impedance analysis after the first formation cycle.—The OEMS measurement showed an onset for the anodic decomposition of VC at ~4.3 V vs. Li/Li$^+$, accompanied by the release of CO_2. To understand the effect of the VC decomposition products formed by VC oxidation on the cathode (e.g., poly(VC) and radicals, see Scheme 2a and 2b) and by VC reduction on the anode (discussed in Reference 5) on cathode and anode impedance growth, we conduct impedance measurements with the gold-wire reference electrode (GWRE) after one formation cycle at 25°C and recharge to 50% SOC (state-of-charge) in LP57 with different concentrations of VC (0, 0.09, 0.17, 0.52, and 2 wt%). The additive concentrations were chosen such that some of the VC concentrations in our lab-scale cells yield VC mass to graphite surface area ratios comparable to those tested in the commercial-scale pouch cell experiments by Burns et al.:[10] 0.09, 0.17, and 2 wt% VC in our lab-scale cells approximately corresponds to 1, 2, and 6 wt% VC in their
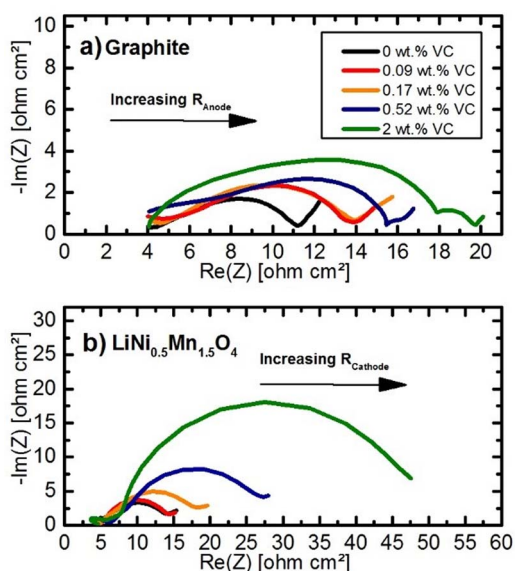
Figure 3. Anode and cathode impedances obtained from graphite/LNMO full-cell with GWRE after one formation cycle and recharge to 50% SOC at 25°C in LP57 with various VC additive concentrations. a) Impedance spectra of the graphite anode of cells containing 0 wt% VC (black lines), 0.09 wt% VC (red lines), 0.17 wt% VC (orange lines), 0.52 wt% VC (blue lines), and 2 wt% VC (green lines); b) analogous impedance spectra of the LNMO cathode. Impedance spectra were measured from 100 kHz to 100 mHz with a current amplitude of 0.6 mA at a temperature of 10°C and at 50% SOC.

commercial-scale cells. In addition, to allow for a better comparison of the resulting anode and cathode impedance, we also conducted our impedance measurements at 10°C, as done in the latter study. Figures 3a and 3b show the Nyquist plots of the graphite and the LNMO electrodes recorded from a graphite/LNMO full-cell with GWRE.

Without VC additive (black lines), the fitted values for the overall resistance of the anode, R_{Anode}, are ∼7 Ωcm² and ∼9 Ωcm² for $R_{Cathode}$. When a small amount of VC (0.09 wt%, red lines) is added to the cells, the overall resistance of the anode increases to ∼10 Ωcm², whereas the impedance of the cathode stays constant at ∼9 Ωcm². When the concentration is increased to 0.17 wt% (orange lines), the impedance of the anode remains at ∼10 Ωcm² while now the impedance of the cathode starts to increase to ∼13 Ωcm². While the anode impedance only increases very little with a further rise in VC concentration, namely to ∼15 Ωcm² for 0.52 wt% VC (blue lines) and to ∼16 Ωcm² for 2 wt% VC (green lines), the cathode impedance increases substantially to ∼22 Ωcm² for 0.52 wt% VC and to ∼41 Ωcm² for 2 wt% VC.

Our interpretation of these observations is as follows: When small amounts of VC (0.09 wt%) are added to the graphite/LNMO cells, it will preferentially be reduced at the graphite anode, leaving no or little VC for oxidation at the LNMO cathode. On the other hand, when higher concentrations of VC are present in the electrolyte (0.17–2 wt%), residual VC remains in the electrolyte after anode SEI formation, allowing for oxidation of VC at the high-voltage LNMO cathode, ultimately leading to cathode impedance growth. As already suggested in previous studies[17] and shown in Scheme 1 (reactions 2a and 2b), the formation of a poly(VC) film on the LNMO cathode is the most likely explanation for the observed impedance increase of the positive electrode shown in Figure 3b. The very high cathode impedance of our lab-scale cell with 2 wt% VC after only one formation cycle indicates that the rapid oxidation of VC at the LNMO cathode potential (shown by OEMS data in Figure 1) leads to the formation of a highly resistive surface film. This would be consistent with the strong capacity fading reported for graphite/LNMO coin cells with 2 wt% VC[14] and will be further examined in the following. These results suggest that the ratio of (anode) additive to graphite surface is
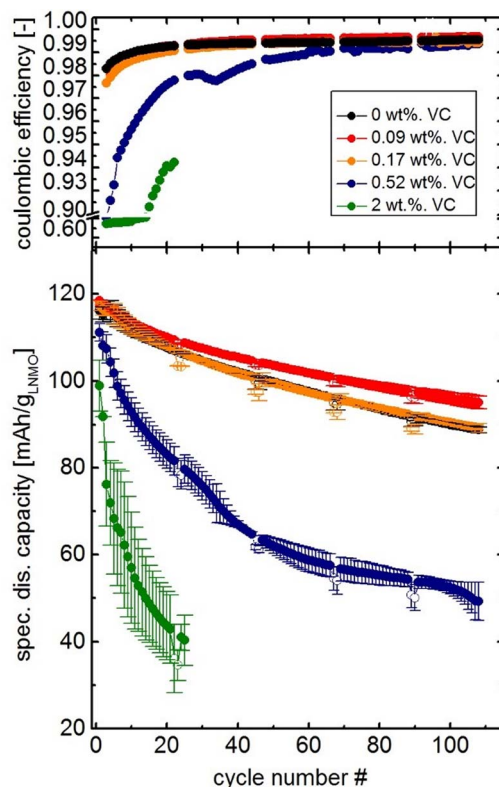

Figure 4. Coulombic efficiency (upper panel) and specific discharge capacity (mAh/g_{LNMO}) (lower panel) of graphite/LNMO cells (without GWRE) over extended charge/discharge cycling at 1C/1C (followed by two 1C/3C cycles after every 20 cycles) and 40°C between 3.5 and 4.8 V in LP57 electrolyte with different VC concentrations: 0 wt% VC (black points), 0.09 wt% VC (red points), 0.17 wt% VC (orange points), 0.52 wt% VC (blue points), and 2.0 wt% VC (green points). The formation of the cells was carried out at 25°C (2 cycles at C/10), while further cycling is done at 40°C. For clarity, the upper panel does not contain data of the two formation cycles and the 1C/3C cycles. The coulombic efficiencies of the two formation cycles (cycle 1 and 2) are given in Table I. Two cells were tested for each electrolyte composition; the figure shows the average of the two cells, with error bars representing the standard deviation. 3C discharge points are filled white for better visibility.

crucial for high-voltage lithium-ion cells, and that a successful use of SEI formers like VC will depend on the competition between additive reduction on the anode and its oxidation on the cathode, as will be explained in more detail in the Discussion section.

Cell cycling at elevated temperatures (40°C) with different concentrations of vinylene carbonate (VC).—As a next step, the influence of different VC concentrations on the cycling behavior at elevated temperatures (40°C) will be investigated. The two main questions are: i) can low concentrations of VC have a beneficial effect on the cycling performance of graphite/LNMO cells, despite the current understanding that VC has a detrimental effect; and, ii) how do the VC oxidation products affect the capacity retention of full-cells. To address these questions, graphite/LNMO cells with different VC concentrations are cycled at 40°C at 1C (CCCV charge, CC discharge; for details see Experimental section) after formation at 25°C (two C/10 cycles). After every twentieth 1C/1C charge/discharge cycle, two 1C/3C charge/discharge cycles are employed in order to gain information about the resistance buildup in the cells, which later on will be compared with the anode/cathode impedance data acquired in repeat experiments using T-cells equipped with a gold wire reference electrode. Figure 4 shows both the specific discharge capacity (in mAh/g_{LNMO}) versus the cycle number (bottom panel) and the coulombic efficiency (top panel) of graphite/LNMO cells with different VC concentrations. For clarity, each dataset shown in Figure 4 contains

the average value of two identical cells (error bars represent the standard deviations between the two cells). Starting from cells which contain no VC (0% VC, black dots), the first discharge capacity at C/10 is ∼117 (±2) mAh/g_{LNMO}, resulting in a first-cycle coulombic efficiency of ∼82%. After 80 cycles, the coulombic efficiency reaches a constant value of ∼99.5% while the discharge capacity remains at ∼88 (±1) mAh/g_{LNMO} after 108 cycles. When adding VC at a commonly used concentration of 2 wt% VC (Figure 4, green dots), the first-cycle discharge capacity at C/10 is only ∼99 (±6) mAh/g_{LNMO}, with a coulombic efficiency of ∼54%, i.e, dramatically lower than in cells with VC-free electrolyte. The capacity loss for cells with 2 wt% VC is very high (57 ±3 mAh/g_{LNMO} after 20 cycles), and the difference in capacity between the last 1C/1C (cycle 25) and the previous 3C/1C cycles amounts to ∼8 (±5) mAh/g_{LNMO} (in contrast to ∼1 (±1) mAh/g_{LNMO} for VC-free electrolyte at the same point), which indicates a dramatic increase in cell impedance. Owing to the already very low capacity after these initial 23 cycles, the test was discontinued here. The poor coulombic efficiency with 2 wt% VC can partly be explained by the early onset of VC oxidation at a cell voltage of ∼4.2 V (i.e., at ∼4.3 V vs. Li/Li$^+$), as evidenced by the OEMS data in Figure 1, since a parasitic oxidation reaction would reduce the coulombic efficiency.

When the concentration of VC is lowered to 0.52 wt% (Figure 4, blue points), the first discharge capacity is ∼111 (±2) mAh/g_{LNMO} and a first-cycle coulombic efficiency of ∼74% is obtained, which is much higher compared to cells with 2 wt% VC (see Table I). After 108 cycles, the discharge capacity is ∼49 (±4) mAh/g_{LNMO} and the coulombic efficiency increases up to 97.5% until cycle 30, where it shows an unexplained drop until cycle 40, and then gradually approaches 99% by the end of the test procedure. Also here, the low coulombic efficiency and capacity retention illustrate the negative impact of VC oxidation products on cell performance. When 0.17 wt% VC are added to the full-cell, a first-cycle discharge capacity of ∼118 (±2) mAh/g_{LNMO} with a first-cycle coulombic efficiency of 82% are observed, quite similar to the case without VC additive (see Table I). Thus, it is not surprising that after 108 cycles, the discharge capacity of ∼88 (±2) mAh/g_{LNMO} is essentially identical to that of the VC-free electrolyte, even though the coulombic efficiency up to cycle 30 is slightly lower (upper panel of Figure 4, orange points). The slightly larger difference between the 1C/1C and the 1C/3C discharge capacity suggests a somewhat higher cell resistance for the 0.17 wt% VC compared to the VC-free electrolyte, which we will correlate with the impedance data in the next section.

So far, the graphite/LNMO cell performance with VC-free electrolyte is clearly superior to VC-containing electrolyte. This observation, however, changes as the VC concentration is lowered to 0.09 wt% (Figure 4, red points), in which case we observe a higher 1st cycle coulombic efficiency (83%), an improved capacity retention (95 (±2) mAh/g_{LNMO} after 108 cycles) compared to cells without VC additive (88 (±1) mAh/g_{LNMO} after 108 cycles), as well as a better coulombic efficiency reaching 99.7% (vs. 99.6%) after 108 cycles.

As shown by Reaction 2a in Scheme 1, the oxidation of VC will release cations into the solution (presumably the cation radicals proposed in Reaction 2a) which will result in one or several of the following processes: i) electroneutrality in the electrolyte requires that lithium ions from the solution must intercalate into the graphite anode (under the reasonable assumption that no intercalation of the radical cations into graphite and/or the PF$_6^-$ anions into LNMO can occur; this is a reasonable assumption, since the amount of C65 is small and as it is not fully graphitized), which would lead to a depletion of
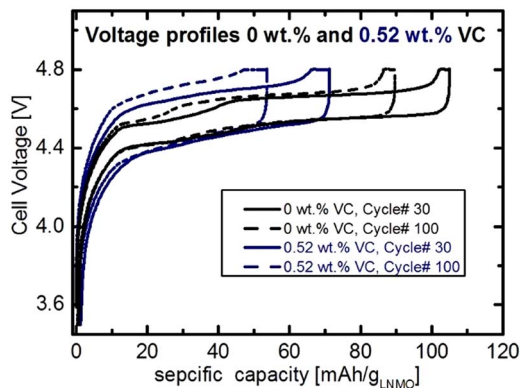
lithium ions in the electrolyte; ii) if the released radical cations stabilize by the release of a proton (as evidenced in our previous study[21]), the proton concentration in the electrolyte would increase (simultaneously decreasing the lithium ion concentration), unless proton intercalation into graphite (during charge) and/or LNMO (during discharge) can occur to a significant degree; iii) VC oxidation and the formation of protons could lead to enhanced dissolution of transition metal ions (as this process is known to correlate with the electrolyte oxidation potential),[37] which – together with oxidation products like HF themselves – could damage the SEI and lead to additional irreversible lithium loss at the anode; and, iv) VC oxidation could lead to impedance growth on anode and/or cathode due to reactions involving VC oxidation products. Regarding the latter, we will see in the following that while the observed impedance growth is substantial, it seems too low to explain the dramatic observed capacity fading. Figure 5 shows the full-cell voltage profiles (E$_{WE}$-E$_{CE}$) for cells with 0 wt% and 0.52 wt% VC after the 30th and 100th cycle. For cells containing 0 wt% VC one can clearly see that the increase in the overpotential during cycling is minor (black solid line vs. black dotted line) and therefore the loss of active lithium is the most likely reason for the capacity fade. Cells with 0.52 wt% VC show an increased polarization, which increases slightly during cycling (blue line vs. blue dotted line). However, as i) the capacity obtained during the constant voltage (CV) step does not increase significantly between cycle 30 and 100 for cells with 0.52 wt% VC, and ii) the voltage profiles for cells with 0.52 wt% VC at the end of the of the constant-current charge still bend upwards, indicating that the cathode is close to complete delithiation, the capacity loss is most likely connected to a loss of active lithium and cannot be solely explained by an increased polarization.

Thus, we believe that the first two mechanisms are the most likely explanation for the observed rapid capacity fading of cells with high concentrations of VC, even though it is currently unclear which one of these processes might be predominant: according to the first mechanism (i), lithium plating would eventually have to occur at the graphite anode and the lithium ion concentration in the electrolyte would get depleted due to a buildup of cationic oxidation products in the electrolyte; according to the second mechanism (ii), protons formed and accumulated in the electrolyte would be expected to corrode the LNMO cathode, resulting in transition metal dissolution and their

Figure 5. Full cell voltage profiles (E$_{WE}$-E$_{CE}$) for cells with 0 wt% and 0.52 wt% VC in graphite/LNMO cells (cycled at 40°C) after cycle 30 and cycle 100.

Table I. Coulombic efficiency of graphite/LNMO cells of the first two formation cycles at C/10 (25°C) for cells with 0, 0.09, 0.17, 0.52, and 2 wt% VC in LP57.

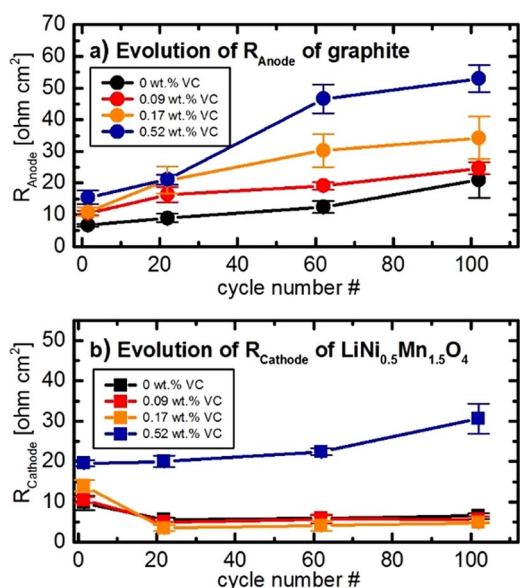| Concentration	0 wt% VC	0.09 wt% VC	0.17 wt% VC	0.52 wt% VC	2 wt% VC
1st cycle	82%	83%	80%	74%	54%
2nd cycle	95%	96%	94%	85%	59%

Figure 6. Evolution of the interfacial electrode resistances (R_{Anode} and $R_{Cathode}$) of graphite/LNMO cells (measured with GWRE) over extended charge/discharge cycling at 1C/1C and 40°C between 3.5 and 4.8 V in LP57 electrolyte with different VC concentrations. a) R_{Anode} of the graphite anode over cycling with 0 wt% VC (black line), 0.09 wt% VC (red line), 0.17 wt% VC (orange line), and 0.52 wt% VC (blue line); b) $R_{Cathode}$ of the LNMO cathode for the same electrolytes. Note that the impedance obtained after the first formation cycle at 25°C and C/10 are included in this figure as cycle 1 (see data shown in Figure 3). Impedance spectra were recorded at 50% SOC and 10°C from 100 kHz to 100 mHz with an amplitude of 0.6 mA. Two cells were tested for each electrolyte composition; the data points show the average of the two cells, with error bars representing the standard deviation.

deposition on the graphite anode. Further studies are currently underway to prove/disprove these hypotheses.

Analysis of the impedance of anode and cathode during cycling.—In this section, we want to investigate the effect of different VC concentrations on the impedance of anode and cathode during cycling. Therefore, the T-cells with GWRE used for the examination of anode and cathode impedance vs. VC concentration after the first formation cycle at 25°C (data shown in Figure 3) were transferred to a 40°C climate chamber where they were was cycled at 1C/1C charge/discharge, The cycling protocol was identical to that used for the cell cycling shown in Figure 4, except that the two 1C/3C charge/discharge cycles after every 20th cycle were omitted. This, however, did not significantly alter the cycle-life: cells equipped with a GWRE and with VC-free electrolyte had a capacity of 87 (±2) mAh/g$_{LNMO}$ after 102 cycles, which is comparable to a capacity of 89 (±1) mAh/g for the cells with the same electrolyte but without reference electrodes (see black symbols in Figure 4). Impedance was measured after the 22nd, 62nd, and 102nd cycle at 50% SOC and 10°C.

Figures 6a and 6b show the overall interfacial resistance of the graphite anode and the LNMO cathode versus cycle number. Note that the data from the first formation cycle are included, where cells were cycled at 25°C.

The anode impedance (Figure 6a) increases roughly linearly with cycle number for cells without VC (black line) and those with 0.09 wt% (red line) and 0.17 wt% VC additive (orange line). For cells with 0 wt% VC, the anode impedance increases from ~7 Ωcm^2 (first cycle) to ~20 Ωcm^2 (102nd cycle). Cells containing 0.09 wt% and 0.17 wt% VC show a similarly gradual impedance increase. For cells with a concentration of 0.17 wt% VC, the impedance increase is slightly higher compared to cells with 0.09 wt% VC, although the initial values for the anode impedance are identical (~10 Ωcm^2). The anode impedance of cells with 0.52 wt% VC increases substantially

during cycling, namely up to ~55 Ωcm^2 after the 102nd cycle. An analogous increase of the graphite anode impedance with increasing VC concentrations was also observed by Burns et al.[10] in commercial-scale graphite/LCO cells for >1 wt.%VC. As will be discussed later, the difference in the VC threshold concentration is due to differences in the electrolyte to graphite surface ratio in commercial-scale vs. lab-scale cells.

Figure 6b shows the interfacial resistance versus cycle number for the LNMO cathode. For cells with 0, 0.09, and 0.17 wt% VC, the impedance decreases after the formation cycle, reaching a constant value of ~5 Ωcm^2 after 20 cycles. In contrast, the LNMO cathode interfacial impedance starts out with a significantly higher value after the first formation cycle (~22 Ωcm^2) for the cells with 0.52 wt% VC and increases with cycle number to ~30 Ωcm^2. We believe that the most likely explanation for the LNMO cathode impedance decrease for low VC concentrations is related to the different temperatures during the first formation cycle (25°C) and the subsequent extended charge/discharge cycling (40°C). During cycling at elevated temperatures, the electrolyte/LNMO interface initially formed at 25°C might be restructured at 40°C by the enhanced solubility of some of the interfacial species (e.g., dissolution of organic interfacial species like poly(VC) or of manganese fluoride produced by reaction with HF traces in the original electrolyte), leading to an impedance decrease. For the cells with 0.52% VC, one could imagine that the relatively high VC concentration has led to a thicker cathode surface film, which cannot be dissolved due to a change in temperature. Further, the on-going cathode impedance growth during cycling could mean that not all VC has been consumed during the initial cycles.

It should be noted that if the content of conductive carbon in the LNMO electrodes is decreased from 5 wt% (used here) to 2 wt%, an increase in LNMO cathode impedance during cycling can be observed even for low VC concentrations. This effect can clearly be attributed to a growing contact resistance at the current collector/electrode interface, as we will show in a future study.[38] However, when 5% carbon black are added to the electrodes (see this study), the increase of the contact resistance is significant.

Discussion

In the following, we will seek to examine why the very low VC concentration of 0.09 wt% in our lab-scale graphite/LNMO cells leads to a clearly improved capacity retention (see Figure 5). This could be understood if these low concentrations of VC are sufficient to form a protective SEI, and if during the first formation cycle, VC reduction at the graphite anode can be completed prior to its oxidation at the LNMO cathode. We will also show that high VC concentrations result in significantly overcharge capacity in the first charging cycle, consistent with the oxidation of the majority of remaining VC at the LNMO cathode. Finally, based on the here observed effect of VC concentration on graphite/LNMO lab-scale cell performance, we will project the VC concentration levels in the electrolyte of commercial-scale cells which would lead to an improved cycling performance of graphite/LNMO cells compared to VC-free electrolyte.

Estimated coverage of VC derived SEI on graphite surface with 0.09 wt% VC additive.—In the following, we want to estimate how many monolayers of poly(VC) can be deposited on the graphite surface by the reduction of all VC contained in the electrolyte with 0.09 wt% VC, i.e., for the concentration which showed the best capacity retention in Figure 4. The purpose of this estimate is to evaluate whether the amount of VC-derived SEI (consisting largely of poly(VC)) at this low VC concentration could yield monolayer thick films, which would be required for surface passivation.

First, we approximate the surface area that can be occupied by one repeat unit of poly(VC), corresponding to the reductive decomposition of one VC molecule.[39] Analogous to Jung et al.,[18] we assume that one adsorbed decomposition product of VC consists of eight atoms (total amount of atoms per poly(VC) repeat unit) and that every atom occupies a square with an average length of a carbon-carbon single

bond of 0.15 nm. Thus, the corresponding area that would be covered by one poly(VC) unit equals to $8 \times (0.15 \text{ nm}^2)^2 = 0.18 \text{ nm}^2$. Taking into account the Avogadro constant ($N_A = 6.022 \cdot 10^{23}$ atoms/mol) and the total surface area of the graphite anodes used in this study ($0.033 \text{ m}^2_{Graphite}$, based on a BET surface area of $\sim 5 \text{ m}^2/g$, a loading of $\sim 7 \text{ mg}_{Graphite}/\text{cm}^2_{electrode}$, and a geometric surface area of 0.95 cm^2), we can now estimate how many moles of VC are required to form one monolayer n_{ML} of poly(VC) on the graphite surface:

$$n_{ML} = \frac{0.033 \text{ m}^2}{N_A \times 0.18 \text{ nm}^2} = 0.307 \text{ } \mu\text{mol/ML} \qquad [1]$$

To obtain the effective number of monolayers of poly(VC) produced on the graphite anode during the first formation cycles, one would need to estimate the fraction of the added moles of VC which are reduced at the anode compared to the fraction which might be oxidized at the cathode. Based on the impedance data in Figure 3b, the LNMO impedance after formation increases only in the cases where the VC concentration is ≥ 0.17 wt%, so that it is reasonable to assume that for cells with 0.09 wt% VC, all VC in the electrolyte is only reduced at the anode, since the oxidation of excess VC on the cathode obviously leads to a highly resistive film (presumably also poly(VC)[17]) on the LNMO cathode. Hence, it should be a reasonable estimate that the total amount of VC in the 0.09 wt% VC electrolyte ($n_{VC} = 0.73 \text{ } \mu\text{mol}_{VC}$ in 60 μL electrolyte) will be reduced at the anode within the first formation cycle to form an SEI layer. In this case, the total number of deposited poly(VC) monolayers N_{ML} in the anode SEI can be estimated as:

$$N_{ML} = \frac{n_{VC}}{n_{ML}} = \frac{0.73 \text{ } \mu\text{mol}_{VC}}{0.307 \text{ } \mu\text{mol/ML}} = 2.4 \text{ ML} \qquad [2]$$

The resulting value on the order of 2–3 monolayer equivalents of poly(VC) could in principle be sufficient to build a passivating VC-derived SEI on the graphite anode. The thickness of this layer, d_{SEI}, can be estimated by assuming that the average monolayer thickness d_{ML} will roughly be the length of a carbon-carbon single bond (0.15 nm):

$$d_{SEI} = N_{ML} \times d_{ML} = 2.4 \text{ ML} \times 0.15 \text{ nm/ML} = \sim 0.4 \text{ nm} \qquad [3]$$

In view of the superior cycling performance with 0.09 wt% VC compared to VC-free electrolyte or electrolyte with higher VC concentrations (see Figure 4) and considering the above estimates, we can finally conclude that a VC concentration of 0.09 wt% is on the one hand sufficiently small to be completely reduced within the first cycle, thus avoiding any detrimental side reactions during subsequent oxidation at the LNMO cathode, and on the other hand still large enough to accomplish adequate passivation of the graphite anode with an average SEI thickness of ~ 0.4 nm. The overall SEI will be thicker than ~ 0.4 nm as also EC and the PF_6^- anion can be reduced after the initial cycles, however a sufficient fraction of the SEI consists of poly(VC) leading to enhanced stability.

Reduction and oxidation of VC considering the half-cell potentials of graphite and LNMO.—The above analysis tacitly assumed that the quantity of VC in the 0.09 wt% electrolyte can be reduced at the graphite anode prior to the onset of VC oxidation at the LNMO cathode during the first formation cycle. That this is indeed feasible can be shown by examining the graphite and LNMO half-cell potentials during the first charging of graphite/LNMO cells. To follow the half-cell potentials during the first charge, a graphite/LNMO cell with 0 wt% VC and a lithium metal reference electrode was used. Figure 7 shows the potential of the graphite anode vs. Li/Li$^+$ and of the LNMO cathode vs. Li/Li$^+$ during the first part of the formation (up to a first charge capacity of 13 mAh/g$_{LNMO}$, which correspond to ~ 1 h of charge at C/10). The dark blue line represents the graphite half-cell potential, while the vertical dashed lines indicate the onset for the VC reduction at ~ 1.8 V vs. Li/Li (blue line) and the reduction of EC at ~ 0.8 V vs. Li/Li$^+$ (red line) taken from References 4 and 5. After a charge capacity of only ~ 0.5 mAh/g$_{LNMO}$ (~ 2 minutes at C/10), the onset potential for the reduction of VC is reached, whereas after a
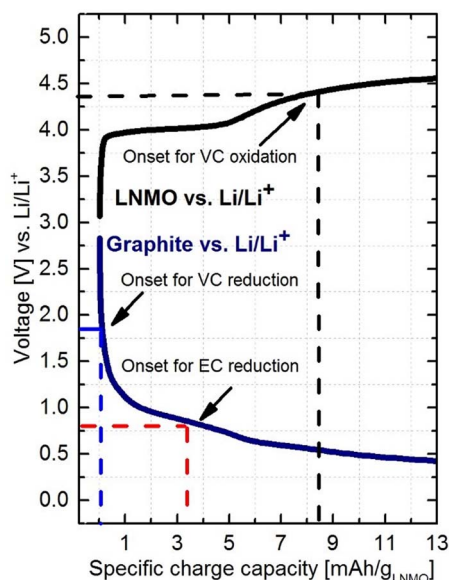

Figure 7. Half-cell potentials of LNMO (black line) and graphite (blue line) vs. Li/Li$^+$ during the first formation cycle at C/10 and 25°C in an VC-free LP57 electrolyte. The vertical dashed lines mark the onset potentials for VC reduction (blue), EC reduction (red), and VC oxidation (black).

total capacity of ~ 4.5 mAh/g$_{LNMO}$ (~ 18 minutes at C/10), the onset potential for EC reduction is reached. At the same time, the half-cell potential of the LNMO cathode (Figure 7, black line) shows a short plateau around ~ 4.0 V vs. Li/Li$^+$ for ~ 6 mAh/g$_{LNMO}$, corresponding to the Mn^{3+}/Mn^{4+} redox couple. Upon further charging, the LNMO potential gradually increases toward its main voltage plateau at ~ 4.7 V vs. Li/Li$^+$, which belongs to the Ni^{2+}/Ni^{3+} redox couple (due to the zoomed-in view of the capacity axis, only the onset for the plateau at 4.7 V vs. Li/Li$^+$ is visible).[40] An potential of ~ 4.3 V vs. Li/Li$^+$, which corresponds to the onset potential for VC oxidation (black vertical line), is reached by the LNMO cathode after ~ 8.5 mAh/g$_{LNMO}$ (i.e., ~ 34 minutes) in this first charge of the graphite/LNMO cell. This means that there are ~ 8 mAh/g$_{LNMO}$ or ~ 30 minutes during the first charge where the graphite potential is already low enough to reduce VC, but where the LNMO potential is still too low to oxidize VC (illustrated by the difference between the vertical blue and black lines in Figure 6). The capacity of ~ 8 mAh/g$_{LNMO}$ can now be compared to the theoretical capacities required for the reduction of different amounts of VC in the electrolyte.

Based on a previous study,[5] the first step in the formation of poly(VC) is most likely the one-electron reduction of VC to the radical anions $\bullet$CH $=$ CH-O-COO$^-$ or $\bullet$CH $=$ CH-O$^-$ (upon release of CO_2), both of which can react with VC to poly(VC). Thus, the formation of poly(VC) would require ≤ 0.5 electrons per VC molecule (depending on the number of repeat units in the poly(VC) product). This implies that the reduction of 0.73 μmol VC in the 0.09 wt% VC electrolyte would require a reductive charge of ≤ 0.010 mAh or, if referenced to the mass of LNMO in the cell (12.9 mg, based on a loading of 13.6 mg$_{LNMO}$/cm^2 and an electrode area of 0.95 cm^2), a charge of ≤ 0.76 mAh/g$_{LNMO}$. Thus, for the 0.09 wt% VC electrolyte, the total amount of VC in the electrolyte can easily be reduced at the graphite anode before the LNMO cathode potential reaches the onset potential for VC oxidation (which occurs at ~ 8 mAh/g$_{LNMO}$ after the VC reduction onset, as discussed before). The same analysis would suggest that even for our VC concentration of 0.52 wt%, the required reductive charge of ≤ 4.5 mAh/g$_{LNMO}$ would still be available prior to reaching an LNMO potential of ~ 4.3 V, which is required to oxidize VC; on the other hand, for 2 wt% VC, the reductive charge which can be passed before the LNMO cathode reaches ~ 4.3 V would likely not suffice to reduce all of the VC in the electrolyte (which would require

≤ 17.3 mAh/g_{LNMO}). While these estimates show that even 0.52 wt% VC in our electrolyte could in principle be reduced at the graphite anode before the LNMO cathode potential is high enough to oxidize VC, the LNMO cathode impedance data after the first formation cycle (see Figure 3b) clearly shows a substantial LNMO impedance increase with VC concentrations ≥ 0.17 wt%, indicating that there is residual VC left in cells with ≥ 0.17 wt% VC after the initial 8.5 mAh/g_{LNMO} charge. These observations fit well to a study by Petibon et al.,[11] who showed that in commercial-scale NMC/graphite pouch cells with 1% wt.VC (corresponding to 0.09 wt% VC in our cells in terms of VC to graphite surface ratio), more than 80% of the initial VC is already consumed after ~50% of the first charge, whereas at the same point, about 4.2 wt% VC is left if the cell originally contained 6 wt% VC (i.e., 0.52 wt% VC in our study). Our results suggest that for the formation of a passivating anode SEI, VC concentrations between 0.09 wt% (no LNMO impedance increase compared to 0 wt% VC, see Figure 3b) and 0.17 wt% (LNMO impedance increase, see Figure 3b) are sufficient. Assuming that the reduction of VC is substantially slowed down once this passivation has been reached, any excess VC would be oxidized at the LNMO cathode once it exceeds a potential of ~4.3 V, as seen in the LNMO impedance for cells with ≥ 0.17 wt% VC.

Overcharge capacities from the anodic decomposition of VC.—
The impedance data in Figure 3b suggest that in the case of higher VC concentrations (≥ 0.17 wt%), a significant fraction of the VC present in the electrolyte must be oxidized in the first cycle at the LNMO cathode. In this case, the additional oxidative current used for the oxidation of VC should increase the first cycle charge capacity.[16,17] Therefore, we want to analyze the first cycle overcharge capacities in graphite/LNMO cells with different amounts of VC. The formation protocol consists of two C/10 charge (CCCV)/discharge (CC) cycles between 3.5 V – 4.8 V cell voltage with a current limit of C/20 for the CV step. Figure 8a shows the first charge of cells with different VC concentrations. For the cells with a concentration of 0 wt% VC
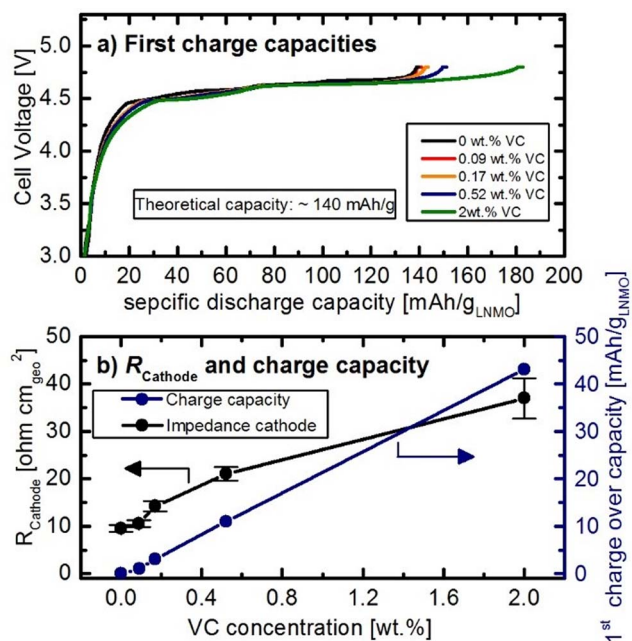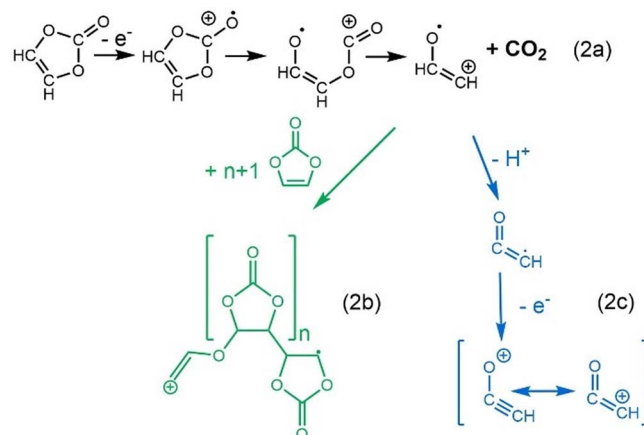
and 0.09 wt% VC, the first charge capacities are ~140 mAh/g_{LNMO} and ~141 mAh/g_{LNMO} (black line and red line in Figure 8a). These values correspond to the theoretical capacity of the LNMO electrode, consistent with our above assumption that no VC oxidation occurs in cells with 0.09 wt% VC. When the concentration of VC is increased to 0.17 wt% VC, the capacity increases to ~144 mAh/g_{LNMO} (yellow line in Figure 8a), indicating that the now occurring electrochemical oxidation of VC causes an additional charge capacity. This is further supported when the concentrations of 0.52 wt% and 2 wt% are taken into account, for which the first charge capacity increases to ~151 mAh/g_{LNMO} and to ~183 mAh/g_{LNMO}, respectively (see blue line and green line in Figure 8a).

In the following, we want to correlate the overcharge capacities arising from VC oxidation (i.e., the first charge capacity minus 140 mAh/g_{LNMO}, which is the first charge capacity of a cell with VC-free electrolyte) to the impedance of the LNMO electrode. In Figure 8b, the first charge capacities (blue symbols, right y-axis) are plotted vs. VC concentration. It is apparent that for VC concentrations ≥ 0.17 wt%, the charge capacity increases proportionally with the VC concentration (i.e., doubling the VC concentration leads to a doubling of the overcharge capacity), which is a clear evidence that excess VC is being oxidized quantitatively during the first charge. The lower than predicted overcharge for the cells with 0.09 wt% VC is in agreement with our assumption that in cells with 0.09 wt% VC, nearly all VC is consumed at the anode before its oxidation can occur. This overall trend fits very well with the LNMO impedance data obtained after the first cycle (see Figure 3b), which are re-plotted in Figure 8b (black symbols, left y-axis), demonstrating that the overcharge capacity and the impedance of the LNMO cathode are correlated. As mentioned before, the impedance increase at the positive electrode can be explained by the formation of poly(VC), which can also be formed during oxidation (see reactions 2a and 2b in Scheme 1). In contrast to the first charge capacity, the cathode impedance grows less severely at high VC concentrations. An explanation for this behavior could be the structural or morphological changes in the poly(VC) layer once a certain thickness has been reached, which might affect the cathode impedance.

The slope of the overcharge capacity vs. VC concentration (see blue line in Figure 8a) corresponds to ~2.4 electrons per VC molecule. However, so far only a ≤ 1 electron per oxidized VC molecule has been proposed (see reactions 2a and 2b in Scheme 1).[17] We thus propose that the larger number of electrons per VC could arise from a further oxidation of the initially produced radical cation (see reaction 2a in Scheme 2), following its stabilization through the release of a proton (see reaction 2c, Scheme 2). The analogous formation of protons during the oxidation of EC/EMC electrolyte has been proposed by Metzger et al.,[21] based on the observation that H_2 is evolved on the

Figure 8. a) First charge of graphite/LNMO cells with 0 wt% VC (black line), 0.09 wt% VC (red line), 0.17 wt% VC (orange line), 0.52 wt% VC (blue line), and 2 wt% VC (green line). The charge is carried out in a constant current constant charge mode (CCCV) with a current limit of C/20 for the CV step. b) First charge capacities of the graphite/LNMO cell and LNMO cathode interfacial impedance, $R_{Cathode}$, after first charge/discharge (data from Figure 3b) vs. VC concentration.

Scheme 2. Extension of the VC oxidation mechanism from Scheme 1 including proton abstraction and a second oxidation step.

anode during electrolyte oxidation, presumably due to the reduction of released protons. After the release of a proton, the intermediate could then be oxidized again, resulting in a mesomerically stabilized cation. Further, this end product of path 2c could again abstract a proton, which would lead to the formation of dicarbon monoxide, a very reactive gas. The so far unexplained 0.4 electrons per molecule VC could be explained by a crosstalk mechanism: oxidation products can diffuse to the anode, where they will be reduced and can then again be oxidized at the cathode, leading to an apparently higher number of electrons per VC. Besides, it is possible that also poly(VC) can be oxidized at high potentials, most likely leading to proton abstraction and additional crosslinking.

Dependence of the graphite anode impedance on the positive electrode (LNMO vs. LFP).—As a next step, we want to understand how the positive electrode affects the impedance of the graphite anode. Therefore, the data of this study is compared with our previous study,[13] where we have investigated the effect of different VC concentrations (0.17 wt% VC and 0.52 wt% VC) on the impedance in graphite/LFP cells. As the upper cutoff potential of the LFP cathode is ~4.1 V vs. Li/Li$^+$ (compared to ~4.9 V vs. Li/Li$^+$ for LNMO), the oxidative decomposition of VC does not occur in graphite/LFP cells, which is in accordance with the LFP cathode impedance being independent from VC concentration (see Figure 8 in Reference 13). To compare the anode impedance data of the graphite/LFP cells from our previous study[13] and the graphite/LNMO cells from the present work, we recalculate the VC concentrations used for both cell chemistries in units of mg$_{VC}$/m$^2_{Graphite}$.

Figure 9 shows graphite anode impedances (R_{Anode}) after the first formation cycle in graphite/LNMO cells (black symbols; data from Figure 3a) and those in graphite/LFP cells (red symbols) vs. the VC concentration in mg$_{VC}$/m$^2_{Graphite}$. As one would expect, the graphite anode impedances for cells with 0 wt% VC are very similar, with a value of ~7 Ωcm^2 for the graphite/LNMO cells and ~5 Ωcm^2 for the graphite/LFP cells. When VC is added to the graphite/LFP cells, the graphite anode impedances increases linearly with VC concentration (to ~16 and ~47 Ωcm^2 for 0.17 and 0.52 wt% VC, respectively), as described previously.[13] Interestingly, the increase of anode impedance between 0 wt% and 0.09 wt% VC in graphite/LNMO cells matches precisely to the linear slope of the graphite/LFP cells. However, at VC concentrations ≥0.17 wt%, a deviation from the linear trend is
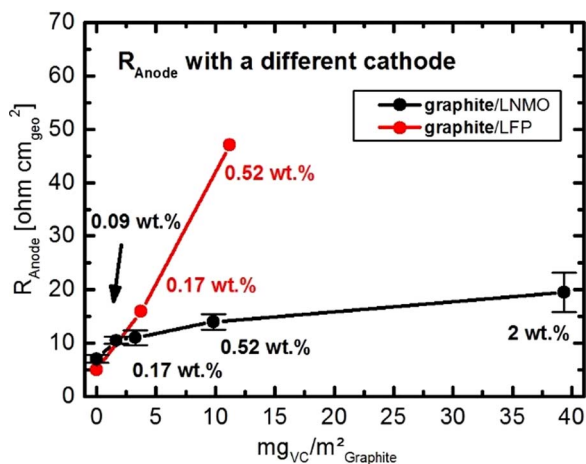

Figure 9. Interfacial resistance of graphite anodes after formation at 25°C in graphite/LNMO cells (this study) compared to graphite anodes in graphite/LFP cells from our earlier study.[13] The VC concentration is recalculated in units of mg$_{VC}$/m$^2_{Graphite}$ to assess for the slightly different areal loadings (namely ~2.6 mAh/cm$^2_{geo}$ in the graphite/LNMO cells and ~2.2 mAh/cm$^2_{geo}$ in the graphite/LFP cells, based on 340 mAh/g$_{graphite}$). The error bars represent the standard deviation between two measurements. All corresponding impedance spectra were recorded at 10°C from 100 kHz to 100 mHz.

observed for graphite/LNMO cells (to ~10 and ~14 Ωcm^2 for 0.17 and 0.52 wt% VC, respectively), i.e., the graphite anode impedance at high VC concentrations is much lower for graphite/LNMO compared to graphite/LFP cells. This effect can be explained by considering the competing reactions at the respective cathode: In graphite/LFP cells, no VC is consumed by the cathode, and the only reaction to occur is the reductive polymerization of VC on the anode, whereas the oxidation of VC on the cathode competes with its reduction in graphite/LNMO cells. Hence, less VC is available for reduction, leading to a lower anode impedance at similar mg$_{VC}$/m$^2_{Graphite}$ amounts. At this point, we would like to mention that the formation of the graphite/LFP cells was carried out at 40°C, while the graphite/LNMO cells were formed at 25°C, which might also affect the resulting anode impedance (measured at 10°C in both cases); however, as the anode impedance for 0 wt% VC is identical for both cell chemistries, and the graphite/LNMO anode impedance with 0.09 wt% VC fits well to the linear relationship between VC concentration and anode impedance in graphite/LFP cells, we believe that the oxidation of VC at the cathode is the major cause for the observed differences between graphite/LNMO and graphite/LFP cells.

Projected performance of graphite/LNMO commercial-scale cells.—The present study clearly proves that VC can enhance the cycling stability of graphite/LNMO cells, in contrast to previous reports. Yet, it also demonstrates that the concentration of VC in graphite/LNMO cells has to be carefully tuned, as the oxidation of only low amounts of VC can already lead to a deterioration of the capacity retention. The optimal VC concentration, corresponding to the amount of VC that can be reduced before the cathode reaches a potential >4.2 V vs. Li/Li$^+$, depends on the ratio of electrolyte to graphite surface area as well as the formation procedure (i.e., the time at potentials where VC reduction, but no oxidation can occur). In our case, the best performance in lab-scale cells is achieved with a concentration of 0.09 wt% VC, which corresponds to ~1 wt% VC in commercial-scale cells as used by Dahn's group (for details on this conversion please refer to Ref. 13). While Burns et al.[7] have shown that already 1 wt% VC leads to a significantly better capacity retention in commercial-scale graphite/LCO and graphite/NMC cells, the cycle life of commercial-scale graphite/NMC cells depends strongly on the amount of VC available.[10] Hence, 1 wt% VC by its own might not be sufficient to achieve an outstanding cycling performance with graphite/LNMO cells. Therefore, a combination of 1 wt% VC with other additives, which are either oxidatively stable or whose oxidation products are not detrimental to cell performance, and which can act as "repair additives" for the VC-derived SEI, would be a feasible combination for commercial-scale graphite/LNMO cells. To assure that diffusion of VC in a lab-scale cell is not the limiting factor when these type of cells are compared to commercial-scale cells we estimate the diffusion times for these two cell types: The diffusion time can be estimated as follows:

$$t = \frac{(x \cdot \tau)^2}{D} \qquad [4]$$

where t is the characteristic diffusion time, x is the length of the diffusion path, τ is the tortuosity of the separator, and D is the diffusion coefficient. A typical value for the liquid diffusion is in the order of 10^{-6} cm^2/s (J. Landesfeind et al.[40]). In our lab test cells, two glass fiber separators have been used (x ≈ 2·200 μm, τ ≈1), yielding a diffusion time on the order of:

$$t = \frac{(400 \, \mu m)^2}{10^{-6} \frac{cm^2}{s}} = 1600 \, s \qquad [5]$$

In a commercial cell the distance between anode and cathode is ~25 μm with an average tortuosity of τ ≈ 4 (see, e.g., J. Landesfeind et al.[41]), yielding an approximate diffusion time constant of:

$$t = \frac{(25 \, \mu m \cdot 4)^2}{10^{-6} \frac{cm^2}{s}} = 100 \, s \qquad [6]$$

As the oxidation of VC would only become possible after $\approx$34 minutes of charge, the rate of VC diffusion to the anode electrode is not limiting. During that initial time period, we believe that VC will be reduced preferentially at the anode, since its reduction potential is substantially higher than that of the EC and EMC solvents in LP57 ($\approx$1.7 V vs. Li/Li$^+$ for VC compared to $\approx$0.9 V for LP57).[5]

Conclusions

In this study, we use a combined on-line electrochemical mass spectrometry (OEMS) and impedance analysis with a micro-reference electrode (GWRE), in order to i) understand the oxidative (in-)stability of the additive vinylene carbonate (VC), and, ii) to investigate the impact of the additive in graphite/LiNi$_{0.5}$Mn$_{1.5}$O$_4$ cells on the interfacial resistance of both anode and cathode. We have shown that the oxidation of VC occurs at an onset potential of $\sim$4.3 V vs. Li/Li$^+$ (by OEMS), which leads to a significant impedance buildup on the LNMO cathode in graphite/LNMO cells. This was shown by monitoring the graphite anode and the LNMO cathode impedance after formation and during extended charge discharge cycling using a micro-reference electrode.

Based on these data, we could conclude that VC oxidation on the cathode is competing with VC reduction on the anode. During the initial charge of graphite/LNMO cells, a charge of $\sim$8 mAh/g$_{LNMO}$ can be passed before the LNMO cathode potential reaches 4.3 V vs. Li/Li$^+$ while the anode potential is already low enough to reduce VC to form an anode SEI. As a consequence, if the total amount of VC in the electrolyte is high enough to form a passivating anode SEI during this initial part of the first charge, but low enough so that all VC is being consumed during the initial anode SEI formation, the capacity retention of cells with a VC-containing electrolyte is superior compared to VC-free electrolyte. In our lab-scale cells, this corresponds to the lowest tested VC concentration of 0.09 wt%. Based on our previously discussed metrics for comparing additives in lab-scale vs. commercial-scale cells, this would translate into a $\sim$1 wt% VC concentration for commercial-scale cells.

Acknowledgment

References

1. E. Peled, *J. Electrochem. Soc.*, **126**, 2047 (1979).
2. R. Imhof and P. Novák, *J. Electrochem. Soc.*, **145**, 3313 (1998).
3. M. Nie, D. Chalasani, D. P. Abraham, Y. Chen, A. Bose, and B. L. Lucht, *J. Phys. Chem. C*, **117**, 1257 (2013).
4. H. Ota, Y. Sakata, A. Inoue, and S. Yamaguchi, *J. Electrochem. Soc.*, **151**, A1659 (2004).
5. B. Zhang, M. Metzger, S. Solchenbach, M. Payne, S. Meini, H. A. Gasteiger, A. Garsuch, and B. L. Lucht, *J. Phys. Chem. C*, **119**, 11337 (2015).
6. M. Nie, J. Demeaux, B. T. Young, D. R. Heskett, Y. Chen, A. Bose, J. C. Woicik, and B. L. Lucht, *J. Electrochem. Soc.*, **162**, 7008 (2015).
7. J. C. Burns, N. N. Sinha, D. J. Coyle, G. Jain, C. M. VanElzen, W. M. Lamanna, A. Xiao, E. Scott, J. P. Gardner, and J. R. Dahn, *J. Electrochem. Soc.*, **159**, A85 (2012).
8. A. Würsig, H. Buqa, M. Holzapfel, F. Krumeich, and P. Novaŕk, *Electrochem. Solid-State Lett.*, **8**, A34 (2005).
9. L. El Ouatani, R. Dedryvère, C. Siret, P. Biensan, S. Reynaud, P. Iratçabal, and D. Gonbeau, *J. Electrochem. Soc.*, **156**, A103 (2009).
10. J. C. Burns, R. Petibon, K. J. Nelson, N. N. Sinha, A. Kassam, B. M. Way, and J. R. Dahn, *J. Electrochem. Soc.*, **160**, A1668 (2013).
11. R. Petibon, J. Xia, J. C. Burns, and J. R. Dahn, *J. Electrochem. Soc.*, **161**, A1618 (2014).
12. R. Petibon, J. Xia, L. Ma, M. K. G. Bauer, K. J. Nelson, and J. R. Dahn, *J. Electrochem. Soc.*, **163**, A2571 (2016).
13. S. Solchenbach, D. Pritzl, E. J. Y. Kong, J. Landesfeind, and H. A. Gasteiger, *J. Electrochem. Soc.*, **163**, A2265 (2016).
14. J. Hoffmann, M. Payne, and J. Li, *ECS Meet. 224, Abstr*, #1106 (2013).
15. H. Lee, S. Choi, H. Kim, Y. Choi, S. Yoon, and J.-J. Cho, *Electrochem. commun.*, **9**, 801 (2007).
16. Y.-M. Song, J.-G. Han, S. Park, K. Lee, and N.-S. Choi, *J. Mater. Chem. A*, **2**, 9506 (2014).
17. Y. Dong, J. Demeaux, and B. L. Lucht, *J. Electrochem. Soc.*, **163**, A2413 (2016).
18. R. Jung, M. Metzger, D. Haering, S. Solchenbach, C. Marino, N. Tsiouvaras, C. Stinner, and H. A. Gasteiger, *J. Electrochem. Soc.*, **163**, A1705 (2016).
19. E. Markevich, G. Salitra, K. Fridman, R. Sharabi, G. Gershinsky, A. Garsuch, G. Semrau, M. Schmidt, and D. Aurbach, *Langmuir*, **30**, 7414 (2014).
20. N. Tsiouvaras, S. Meini, I. Buchberger, and H. A. Gasteiger, *J. Electrochem. Soc.*, **160**, A471 (2013).
21. M. Metzger, B. Strehle, S. Solchenbach, and H. A. Gasteiger, *J. Electrochem. Soc.*, **163**, A798 (2016).
22. M. Metzger, C. Marino, J. Sicklinger, D. Haering, and H. A. Gasteiger, *J. Electrochem. Soc.*, **162**, A1123 (2015).
23. M. Klett, J. A. Gilbert, S. E. Trask, B. J. Polzin, A. N. Jansen, D. W. Dees, and D. P. Abraham, *J. Electrochem. Soc.*, **163**, A875 (2016).
24. R. Jung, M. Metzger, F. Maglia, C. Stinner, and H. A. Gasteiger, *J. Electrochem. Soc.*, **164**, A1361 (2017).
25. J. A. Seel and J. R. Dahn, *J. Electrochem. Soc.*, **147**, 892 (2000).
26. W. Märkle, N. Tran, D. Goers, M. E. Spahr, and P. Novák, *Carbon*, **47**, 2727 (2009).
27. M. Metzger, J. Sicklinger, D. Haering, C. Kavakli, C. Stinner, C. Marino, and H. A. Gasteiger, *J. Electrochem. Soc.*, **162**, A1227 (2015).
28. M. Itagaki, N. Kobari, S. Yotsuda, K. Watanabe, S. Kinoshita, and M. Ue, *J. Power Sources*, **148**, 78 (2005).
29. X. Zhang, J. K. Pugh, and P. N. Ross, *J. Electrochem. Soc.*, **148**, E183 (2001).
30. O. Borodin, W. Behl, and T. R. Jow, *J. Phys. Chem. C*, **117**, 8661 (2013).
31. J. Self, C. P. Aiken, R. Petibon, and J. R. Dahn, *J. Electrochem. Soc.*, **162**, A796 (2015).
32. C. P. Aiken, J. Self, R. Petibon, X. Xia, J. M. Paulsen, and J. R. Dahn, *J. Electrochem. Soc.*, **162**, A760 (2015).
33. L. E. Downie, S. Hyatt, and J. R. Dahn, *J. Electrochem. Soc.*, **163**, A35 (2016).
34. L. Xing, W. Li, C. Wang, F. Gu, M. Xu, C. Tan, and J. Yi, *J. Phys. Chem. B*, **113**, 16596 (2009).
35. T. Li, L. Xing, W. Li, Y. Wang, M. Xu, F. Gu, and S. Hu, *J. Power Sources*, **244**, 668 (2013).
36. J. Landesfeind, D. Pritzl, and H. A. Gasteiger, *J. Electrochem. Soc.*, **164**, A1773 (2017).
37. D. H. Jang and S. M. Oh, *J. Electrochem. Soc.*, **144**, 3342 (1997).
38. D. Pritzl, A. Bumberger, M. Wetjen, S. Solchenbach, J. Landesfeind, and H. A. Gasteiger, *Manuscr. prep.*.
39. A. L. Michan, B. S. Parimalam, M. Leskes, R. N. Kerber, T. Yoon, C. P. Grey, and B. L. Lucht, *Chem. Mater.*, **28**, 8149 (2016).
40. B. Li, L. Xing, M. Xu, H. Lin, and W. Li, *Electrochem. commun.*, **34**, 48 (2013).
41. A. Ehrl, J. Landesfeind, W. A. Wall, and H. A. Gasteiger, *J. Electrochem. Soc.*, **164**, A826 (2017).